Acta Geotechnica (2022) 17:65–79
https://doi.org/10.1007/s11440-021-01200-1

RESEARCH PAPER

Instability and liquefaction flow slide of granular soils: the role of initial shear stress

J. Yang[1] · L. B. Liang[1] · Y. Chen[1]

Received: 4 August 2020 / Accepted: 30 March 2021 / Published online: 3 May 2021

Abstract

Loose granular soil, when subjected to shearing, may collapse rapidly to large strains with a very low residual strength. This flow-type failure, known as flow slide or flow liquefaction, is a major concern in geotechnical applications involving slopes, dams and embankments. A fundamental understanding of the flow liquefaction phenomenon has been established through extensive laboratory experiments on isotropically consolidated sand samples over the past decades. In real situations, however, the element of soil in a slope or dam is not under the isotropic consolidation, but is subjected to a static, driving shear stress prior to external loading. What role played by this static shear stress in the initiation of flow liquefaction is an issue of importance but is not yet fully understood. This paper presents new data from a specifically designed experimental program along with analysis in a sound theoretical context. A marked finding of the study is that the gradient of the flow liquefaction line—which indicates the onset of flow slide in the stress space—is almost uniquely related to the initial state parameter defined in the critical state theory, regardless of the presence or absence of initial shear stress. Based on the characteristics of the observed behavior, an alternative definition for the factor of safety against flow failure is put forward, which takes proper account of the key factors involved and thus is more rational in certain aspects than the conventional one used in engineering practice.

Keywords Flow slide · Granular material · Instability · Liquefaction · Shear behavior

List of symbols

A, B	Parameters in Eq. (3)
ACR	Anisotropic consolidation ratio
e	Void ratio after consolidation
e_Γ	Critical state parameter in Eq. (5)
K_0	Earth pressure coefficient at rest
K_c	Principal stress ratio
M	Critical stress ratio
p	Mean effective stress in standard triaxial setting
p_a	Reference pressure (atmospheric pressure)
q	Deviatoric stress in standard triaxial setting
R_{FL}	Resistance to flow liquefaction
S_{IC}	Shear stress increment
S_0, s_d	Initial shear stress and applied shear stress
s_p, s_u	Undrained strength at peak state and critical state
α, β	Parameters in Eq. (7)
ε_1, ε_3	Major and minor principal strain
ε_a	Axial strain in triaxial test
ϕ_{cs}	Critical state friction angle
η_{FLL}	Stress ratio corresponding to flow liquefaction line
λ	Critical state parameter in Eq. (5)
ψ	State parameter
ψ_0	Initial state parameter (prior to shearing)
σ_1, σ_3	Major and minor principal stress

1 Introduction

Flow slide or flow liquefaction is a phenomenon in which loose granular soil, when subjected to shear, undergoes a sudden loss of strength and a rapid development of deformation, accompanied by a quick buildup of pore water pressure. It is essentially an instability behavior and can be triggered by either static or cyclic loading. The consequences of this flow-type failure are often dramatic and devastating. A classic example is the collapse of the Fort Peck dam in the USA [4], which resulted in flow slides of several million cubic meters of the dam material and

✉ J. Yang
junyang@hku.hk

[1] Department of Civil Engineering, The University of Hong Kong, Hong Kong, China

eight deaths. Another notable case is the massive slides during construction of the Nerlerk sand berm in the Beaufort Sea [25], which led to the abandonment of the project and a financial loss of over 100 million US dollars. Most recent examples include the catastrophic failures of large tailings dams in Brazil [21]. Given the potentially catastrophic consequences, considerable efforts have been devoted to investigate the phenomenon in the past decades, mainly through well-controlled laboratory experiments on saturated sand samples; and a framework of understanding has been established (*e.g.* [4, 5, 10, 14, 16, 19, 23–25, 27, 29, 30, 34, 35, 42]).

Central to the current understanding is the existence of a critical state line in the stress space (Fig. 1), which is the locus of ultimate states of shear failure, termed as steady state or critical state [23, 32], and the existence of a flow liquefaction line, which links the peak in the stress path and the origin. The two lines in the stress space define a zone of potential instability in which loose sand tends to become unstable when a perturbation is imposed. In this context, the flow liquefaction line is also referred to as instability line and Hill's classic instability criterion [12] can be applied to explain the initiation of failure (*e.g.* [3]. Using the standard triaxial notations, the critical state can be analytically defined as:

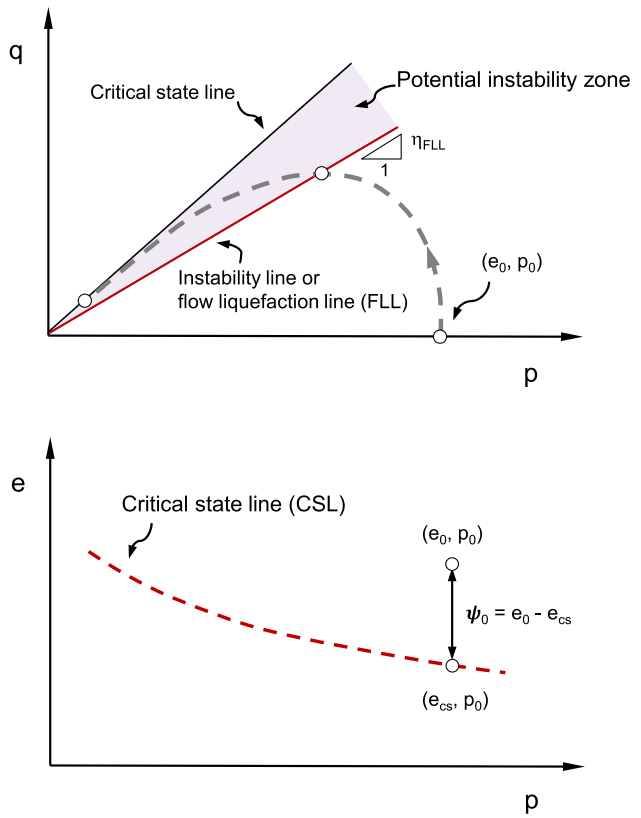

Fig. 1 Undrained loading of loose saturated sand leading to flow liquefaction

$$dp = 0; dq = 0; d\varepsilon_v = 0; d\varepsilon_q \neq 0 \tag{1}$$

where $p = (\sigma_1 + 2\sigma_3)/3$ is the mean normal stress and $q = (\sigma_1 - \sigma_3)$ is the deviatoric stress, with σ_1 and σ_3 as the principal stresses; $\varepsilon_v = (\varepsilon_1 + 2\varepsilon_3)$ is the volumetric strain and $\varepsilon_q = 2(\varepsilon_1 - \varepsilon_3)/3$ is the deviatoric strain. Equation (1) states that at the critical state the deviatoric strain continues indefinitely without changes in mean effective stress, deviatoric stress and volume. Note that both stress and strain quantities are assumed positive in compression and all stress components throughout this paper are considered effective. The instability criterion is hence given as:

$$d^2W = d\sigma_{ij}d\varepsilon_{ij} = (dpd\varepsilon_v + dqd\varepsilon_q) \leq 0 \tag{2}$$

More attention deserves to be paid to the notion that the flow liquefaction line is not an *intrinsic* property but depends on both void ratio and mean effective stress. Its gradient can be related to the initial state parameter (ψ_0) of the soil in an exponential form [35]:

$$\eta_{FLL} = \left(\frac{q}{p}\right)_{FLL} = \frac{M}{B}\exp(A\psi_0) \tag{3}$$

where M is the gradient of the critical state line; and A and B are two soil-specific parameters. As shown in Fig. 1, the state parameter is a measure of how far the material state is from the critical state in terms of density by collectively accounting for the influence of void ratio and mean effective stress [1]. The state dependence described in Eq. (3) has been confirmed by laboratory experiments on different granular materials (*e.g.* [17, 24, 31] and by numerical simulations using the discrete element method (*e.g.* [8, 9, 13]. A significant implication of the relationship is that a granular soil at a relatively dense state also has the potential for liquefaction as long as the confining stress is sufficiently high.

Most of the studies on flow liquefaction have tended to focus on sand specimens sheared under the isotropic consolidation condition. This condition, however, does not properly replicate the in situ stress condition typical for slopes and dams—in which *a static, driving shear stress* exists in the element of soil prior to external loading (Fig. 2). While this stress condition has been recognized for a long (*e.g.* [18], it is not yet extensively studied. One of notable studies in recent years is that of Fourie and Tshabalala [11], who reported an investigation of the failure of a tailings dam in South Africa. They showed that the use of the friction angle corresponding to the flow liquefaction line determined from isotropically consolidated specimens would lead to unreasonably low values of factor of safety. Based on laboratory tests on K_0-consloidated and isotropically consolidated specimens of the tailings material, they concluded that the flow liquefaction line determined from K_0-consloidated specimens is positioned *steeper* in the

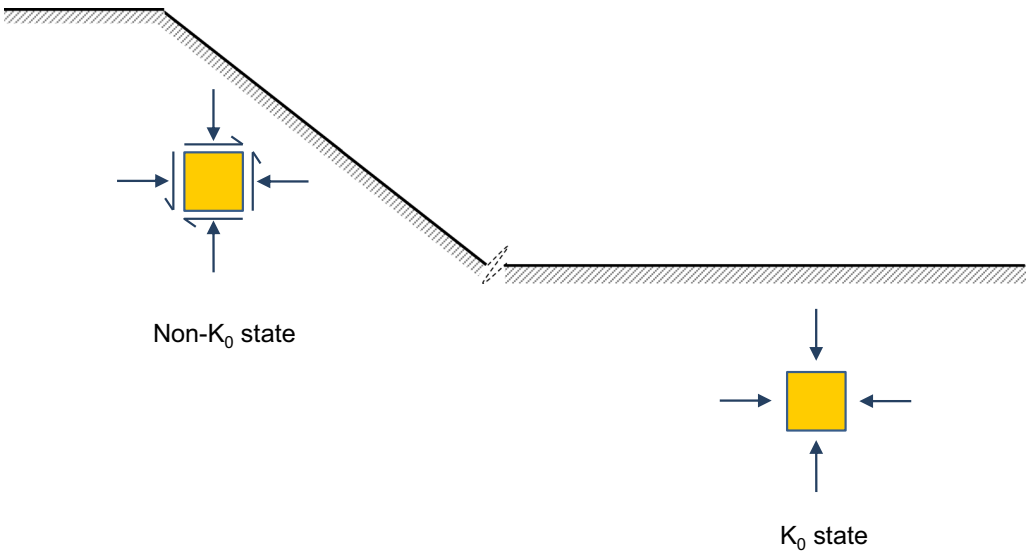

Fig. 2 Schematic illustration of stress states in sloping and level ground conditions

stress space, thus leading to a larger friction angle and a higher factor of safety. This conclusion is somehow counterintuitive and confusing—because it suggests that the presence of an initial shear stress is beneficial to the safety of slopes and dams. Later on, Chu and Wanatowski [7] also reported data from undrained shear tests on K_0-consolidated sand specimens, but their results showed that the stress ratio corresponding to the onset of instability does not differ appreciably from that for isotropically consolidated specimens.

The divergent views in the literature indicate that the problem is complex and is not yet fully understood. This divergence also reflects to some extent the uncertainty involved in K_0-consolidation tests. In carrying out such tests in soil mechanics laboratory, the lateral strain caused by a stress increment needs to be carefully controlled to fulfill the condition of no lateral deformation; however, the accuracy of lateral strain measurement is always a concern. Adding to this uncertainty is that the K_0 value of a granular soil is dependent on its initial void ratio—that is, different K_0 values may correspond to different void ratios or vice versa. Since the undrained behavior of granular soil is sensitive to changes in void ratio, one may speculate that the observed differences in laboratory tests on K_0-consolidated and isotropically consolidated specimens are associated with differing void ratios of the specimens.

Another critical concern is that K_0-consolidation essentially represents *level ground* conditions in the free field where no static, driving shear stress acts on the horizontal plane of the soil element and, thereby, no potential for flow failure exists. For *sloping ground* conditions, the element of soil is, however, subjected to a static, driving shear stress before any loading effect is developed. To simulate the sloping ground conditions in the laboratory, it is more rational to apply a drained loading to the soil specimen to generate an initial shear stress [40, 41]. This loading process can be regarded as a general anisotropic condition for which the magnitude of the initial shear stress can be related to the anisotropic consolidation ratio (ACR) defined below:

$$\mathrm{ACR} = \frac{q_0}{p_0} \tag{4}$$

where q_0 is the deviatoric stress and p_0 is the mean effective stress prior to loading. Evidently, the steeper the slope, the higher the initial shear stress and the larger the ACR value. The limiting case of ACR = 0 represents the isotropic consolidation (i.e., no initial shear stress). Alternatively, the principal effective stress ratio after the general anisotropic consolidation, defined as $K_c = \sigma_1/\sigma_3$, can also be used. It can be readily shown that K_c and ACR are related to each other.

With the above concerns in mind, this paper presents a study with the aim to explore the role of initial shear stress through a specifically designed experimental program along with analysis in the critical state framework. Particular attention has been given to the following fundamental questions:

(a) Whether the flow liquefaction line (i.e., the instability line), determined under the general anisotropic consolidation condition, is dependent on both void ratio and mean effective stress?
(b) If yes, can this state dependence be described by a relationship between the gradient of the flow liquefaction line and the state parameter?

(c) Whether this relationship, if existing, differs from that established under the isotropic consolidation condition?

From the practical point of view, seeking answers to these questions is a necessary step toward the development of safer and more rational methods for evaluation of instability and liquefaction potential of dams and slopes. From the theoretical point of view, the comprehensive data sets can be a useful reference for validation and calibration of advanced constitutive models for granular materials and for the development of a better understanding of the physics involved.

2 Laboratory experimental program

All experiments presented here were undrained triaxial compression tests, conducted on Toyoura sand, a uniform quartz sand that has been widely used in soil mechanics laboratories for various purposes. Its mean particle size (D_{50}) is 0.203 mm and the coefficient of uniformity (C_u) is 1.474, with 0% fines content; its particles are subrounded to subangular. Each specimen, measured 71.1 mm in diameter and 142.2 mm in height, was prepared by the moist tamping method with the under-compaction technique. Compared with several other methods for sample preparation [26], the method has the advantage of producing a wide range of void ratios with good uniformity [14]. Each specimen was carefully saturated in two stages: initially by flushing the specimen with carbon dioxide and de-aired water, and then by applying a back pressure (300–400 kPa with the B-check. A specimen with a B-value greater than 0.95 was considered saturated, and for most specimens their B-values were greater than 0.99. After saturation, the specimen was either isotropically or anisotropically consolidated to the target state, from which undrained compression was applied with a specific strain rate (0.5%/min). The strain-controlled tests allowed a reliable data collection for the post-peak response, thus giving a well-defined stress path and stress–strain relation. The post-consolidation void ratio of each specimen was determined by carefully measuring the water content at the end of the test so as to achieve a high level of accuracy [42]. In doing that, the following procedure was taken: (1) the cell pressure was released and the triaxial chamber was dissembled after the termination of a test; (2) the total weight of the wet sand sample together with the membrane and O rings was measured; (3) the membrane and O rings were separated from the sand sample and their dry weight was determined; and (4) the sand sample was dried in an oven and its dry weight was measured.

To produce systematic data sets capable of rendering answers to the questions raised, a range of ACR values, varying from zero to unity, was applied, and the consolidation pressure was also varied over a broad range. While focus of this study was placed on loose sand specimens susceptible to liquefaction, a number of tests were also conducted on samples at medium dense to dense state so as to gain a comprehensive view. Table 1 summarizes the test series. For limited space, selected test results are presented and discussed in the following sections.

3 Overall behavior and influence of initial shear stress

Figure 3 shows the results of four triaxial tests in terms of stress path and stress–strain curve, where the four specimens were isotropically consolidated to the same stress level but differing void ratios. While the influence of void ratio is well recognized, attention deserves to be paid to the sensitivity of the undrained behavior of sand to the post-consolidation void ratio. Under otherwise identical conditions, a small variation in void ratio can lead to a markedly different response, from non-liquefiable ($e_0 = 0.878$) to highly liquefiable ($e_0 = 0.946$). The behavior in between these two extreme cases ($e_0 = 0.894$)—characterized by a peak strength followed by a limited period of strain softening and then a continuous dilation to high strength—is known as limited flow or limited liquefaction. Although no full liquefaction occurs in such cases, caution should be exercised that the strains associated with the local minimum strength (referred to as quasi-steady state in the literature) are often sufficiently large ($> 5\%$) to cause damage to earth structures.

The phenomenon of quasi-steady state has been consistently observed in laboratory experiments (*e.g.* [29]. Nevertheless, there has been a concern about whether it is a true behavior or a test-induced phenomenon [28, 43]—the question behind the phenomenon is: How can a sand sample, after failure, regain strength with further loading, and the regained strength can even be higher than its peak strength? Recent studies from the micromechanical perspectives [31, 36] provide some insights into the nature of the state—that is, the quasi-steady state is a real material response marking the transition from a metastable to a stable microstructure of granular assemblies under the *constant volume* shear. The phenomenon of quasi-steady state can also occur in anisotropically consolidated samples, as shown in Fig. 4. All the three specimens underwent brittle failure, reached the local minimum strength at quite large strains ($\sim 15\%$), and then regained strength upon further loading. The existence of the quasi-steady state implies that vanishing second-order work specified in

Table 1 Summary of testing series

Test series	e_0	p_0 (kPa)	ACR	K_c
Series I-a	0.951	100	0	1
	0.936	100	0	1
	0.924	100	0	1
	0.905	100	0	1
	0.893	100	0	1
	0.881	100	0	1
	0.867	100	0	1
	0.848	100	0	1
	0.919	100	0	1
Series I-b	0.887	200	0	1
	0.941	200	0	1
	0.908	300	0	1
	0.922	300	0	1
	0.943	300	0	1
	0.885	300	0	1
Series I-c	0.910	500	0	1
	0.928	500	0	1
	0.894	500	0	1
	0.878	500	0	1
	0.946	500	0	1
Series II	0.932	300	0.273	1.30
	0.956	300	0.273	1.30
	0.950	500	0.273	1.30
Series III	0.928	92	0.545	1.66
	0.909	100	0.545	1.66
	0.894	100	0.545	1.66
	0.880	100	0.545	1.66
	0.864	100	0.545	1.66
	0.916	100	0.545	1.66
	0.906	300	0.545	1.66
	0.947	300	0.545	1.66
	0.939	500	0.545	1.66
Series IV	0.923	100	0.923	2.33
	0.889	100	0.923	2.33
	0.919	100	0.923	2.33
	0.918	260	0.923	2.33
	0.925	300	0.923	2.33
	0.911	300	0.923	2.33
	0.942	300	0.923	2.33
	0.905	400	0.923	2.33
	0.934	500	0.923	2.33
	0.923	100	1	2.5

e_0 = post-consolidation void ratio; p_0 = mean effective stress after consolidation; ACR = anisotropic consolidation ratio; K_c = principal stress ratio

Eq. (2) is not sufficient for the occurrence of instability—because while the condition in Eq. (2) is satisfied at this state, further loading beyond the state leads to a stable, dilative response.

The importance of void ratio was also observed on anisotropically consolidated sand specimens. Shown in Fig. 5 are test results for two specimens anisotropically consolidated to the same stress state (ACR = 0.545) but different void ratios. The specimen at a void ratio of 0.926 was brought to liquefaction shortly after the application of loading, whereas the specimen at a void ratio of 0.864 exhibited a strongly dilative response and achieved a significantly high strength at large strains. Similar results were obtained from testing another pair of anisotropically consolidated specimens at a higher ACR value (0.923), as shown in Fig. 6, where the contrasting response was due to a small change in void ratio. These tests underline the importance of accurate determination of the post-consolidation void ratio in laboratory study of sand behavior.

Of more interest here is how the presence of initial shear stress influences liquefaction resistance. Compared with the case of no initial shear stress, the increase in shear stress required to initiate liquefaction—which can be regarded as the resistance to flow liquefaction—is significantly lower when an initial shear stress is present. To make the point clear, a series of tests was designed to eliminate the effects due to differing void ratios and confining stresses, and the results are shown in Fig. 7. The uniqueness of Fig. 7 is that all the three samples were consolidated to almost the same state in terms of mean effective stress and void ratio, but with different ACR values. In the absence of initial shear stress (ACR = 0), the increase in shear stress required to initiate liquefaction was measured to be approximately 108 kPa. When an initial shear stress was present at ACR = 0.545, the increase in shear stress required to initiate liquefaction was dramatically reduced to about 42 kPa, and it was further reduced to about 14 kPa at a higher shear stress level (ACR = 0.923). Since all the three tests were conducted under otherwise similar conditions, the results in Fig. 7 provide convincing evidence that the resistance against the onset of instability and liquefaction reduces with increasing initial shear stress level. Similar observation has been observed by Jefferies and Been [16] from laboratory tests on K_0-consolidated specimens and by Kramer and Seed [18] from load-controlled triaxial tests on a river sand. Compared with strain-controlled tests, load-controlled tests are not able to provide reliable post-peak measurements and thus do not allow analysis in the critical state context.

In addition to the effect on liquefaction resistance, several features in Fig. 7 are worth noting: (a) Flow failure or instability was initiated at very low strains for all samples ($< \sim 0.5\%$, see Fig. 7b), and the strain level at the onset of instability tended to decrease with increasing ACR; (b) the excess pore water pressures in all samples

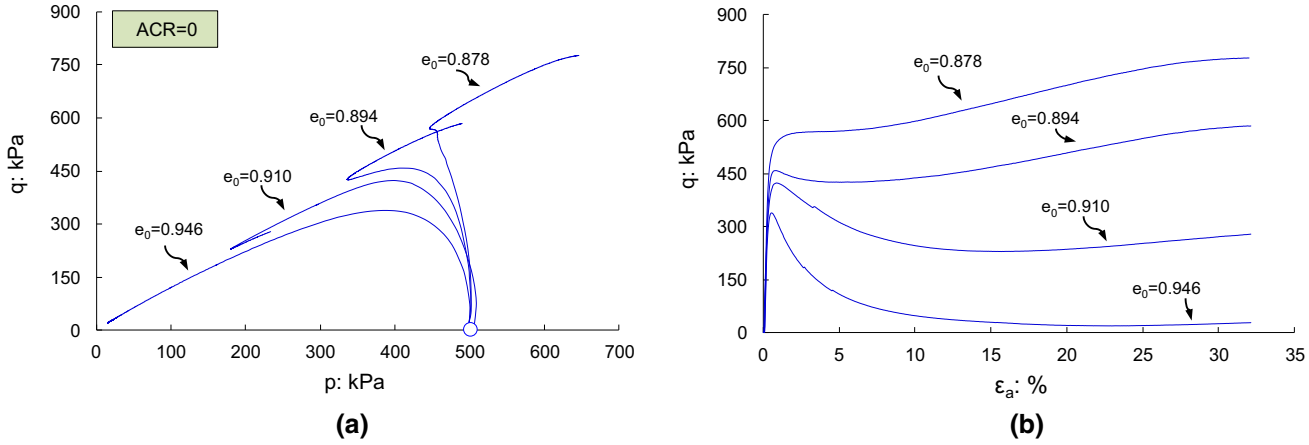

Fig. 3 Undrained shear behavior of isotropically consolidated sand specimens at varying void ratios: **a** stress path; **b** stress–strain relation

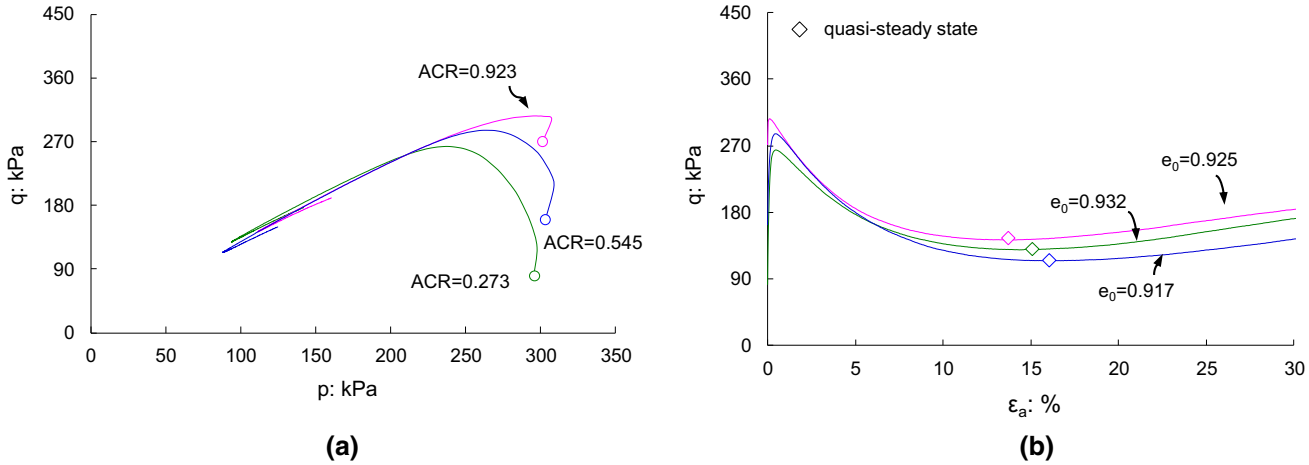

Fig. 4 Quasi-steady state observed on anisotropically consolidated sand specimens at various ACR values: **a** stress path; **b** stress–strain relation

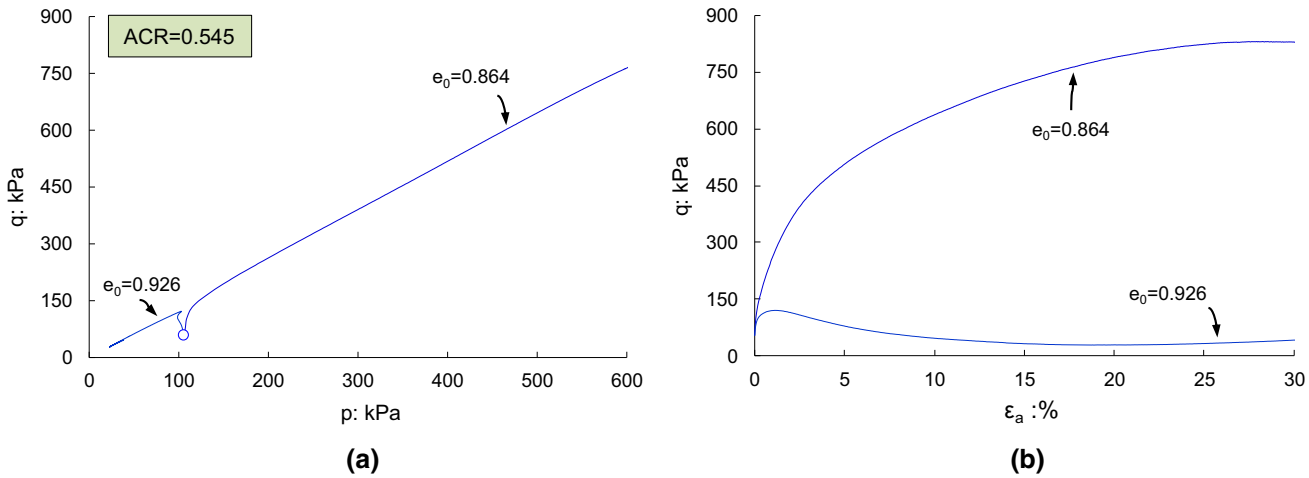

Fig. 5 Undrained shear behavior of anisotropically consolidated sand specimens (ACR = 0.545) at different void ratios: **a** stress path; **b** stress–strain relation

were built up continuously during undrained shear, showing no abrupt changes at the onset of instability, but the magnitudes of pore water pressures were significantly affected by the initial shear stress level (Fig. 7c); and

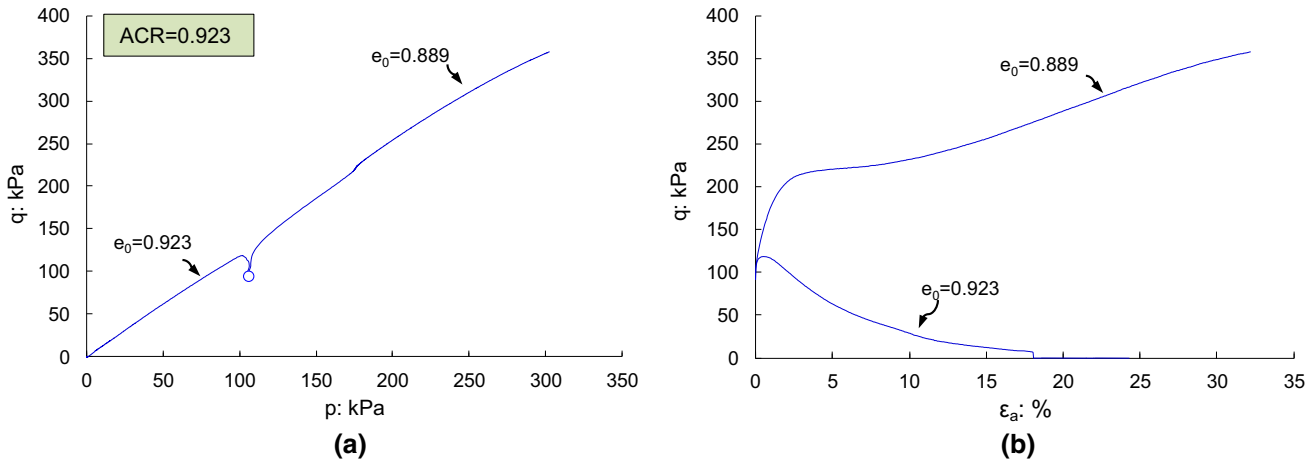

Fig. 6 Undrained shear behavior of anisotropically consolidated sand specimens (ACR = 0.923) at different void ratios: **a** stress path; **b** stress–strain relation

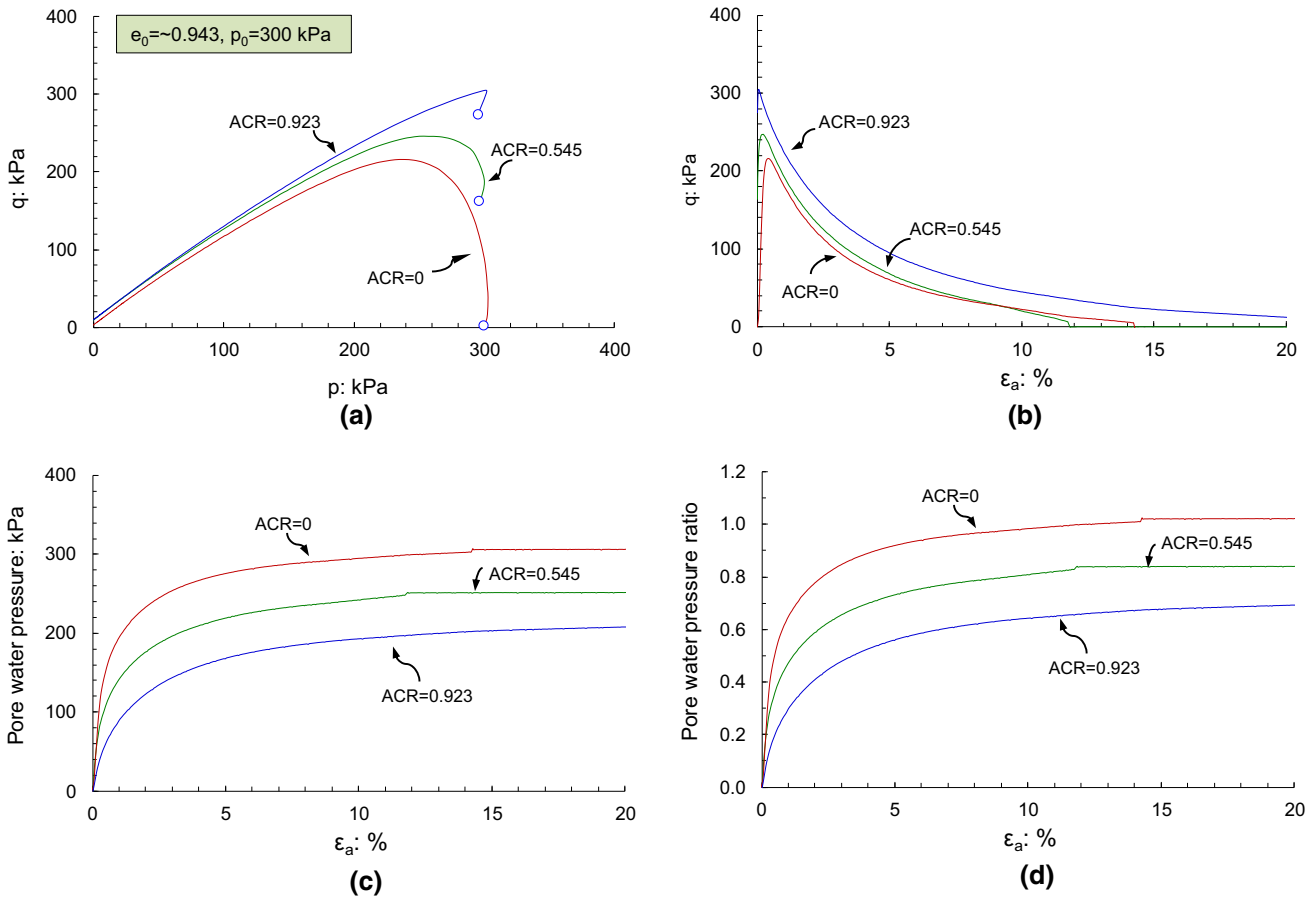

Fig. 7 Influence of initial shear stress on undrained shear behavior of loose sand: **a** stress path; **b** stress–strain relation; **c** pore water pressure response; **d** pore water pressure ratio

(c) the pore water pressure ratio, defined as the pore water pressure divided by the mean effective stress at the end of consolidation, approached unity at large strains in the case of no initial shear stress, but it was not able to achieve the limiting value in the presence of initial shear stress (Fig. 7d). To make these points clearer, the magnitude of shear stress required to initiate failure, the strain at the onset of failure, and the maximum pore water pressure ratio attained for all the three tests are shown as a function of ACR in Fig. 8a–c, respectively. Note that in the case of

ACR = 0.923, flow failure or instability was initiated at an *extremely low* strain (∼ 0.05%)—one order of magnitude less than that commonly reported in the literature. This result implies that the displacements in associated with the onset of flow slides of steep slopes in field conditions would be very small such that any deformation-based precautionary warning would be difficult, if not impossible. It also explains why the occurrence of flow slides is historically known as *spontaneous* liquefaction [4]. As far as the excess pore water pressure is concerned, the maximum value attained in the case of ACR = 0.923 was only 70% of that in the case of no initial shear stress (ACR = 0).

The observed effect of initial shear stress on pore water pressure generation due to monotonic loading is in consistent with that observed by some researchers from undrained cyclic tests. For ease of reference, Fig. 9 shows the results of cyclic tests on two Toyoura sand samples at a similar initial state [41]: one was subjected to isotropic consolidation (i.e., no initial shear stress) and the other was subjected to a drained loading induced shear stress (∼ 36 kPa) before the application of cyclic loading. Clearly, the presence of an initial shear stress can significantly prevent the generation of pore water pressure as observed in monotonic tests. In the absence of initial shear stress, the pore water pressure built up to the level of effective confining stress shortly after 4 cycles of loading, whereas it was unable to rise to 20% of the effective confining stress even after 20 cycles of loading. The result suggests that the commonly used liquefaction criterion, i.e., the occurrence of liquefaction is defined as the state at which the excess pore water pressure ratio equals unity (*e.g.* [15], can be misleading in situations where a significant initial shear stress is present. For such situations, the development of large deformation is considered a more rational criterion.

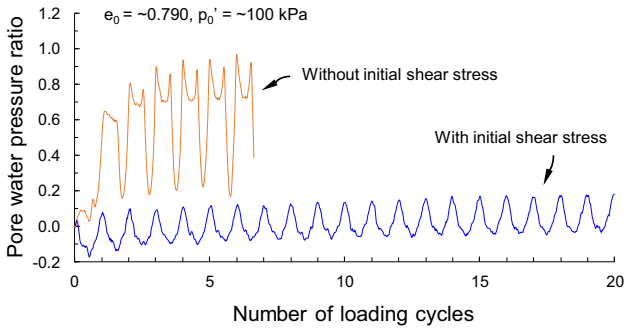

Fig. 9 Influence of initial shear stress on pore water pressure generation under cyclic loading (after [40, 41])

4 State-dependent flow liquefaction line

Now, it is interesting to examine how the initiation of flow liquefaction or the onset of instability is affected by the initial state of soil in the presence of initial shear stress. Figure 10a shows data from eight tests in terms of the slope of the flow liquefaction line (η_{FLL}), i.e., the stress ratio at the onset of instability, as a function of post-consolidation void ratio (e_0). For all the tests, no initial shear stress was applied before undrained shear (i.e., ACR = 0); five of them were under the confining stress of 100 kPa, and three of them were under a much higher confining stress of 500 kPa. Two aspects are evident from the plot: (a) under a given confining stress, η_{FLL} tends to decrease with increasing void ratio, meaning that the specimen at a looser state is more prone to the initiation of flow liquefaction; and (b) for a given void ratio, the specimen at a higher

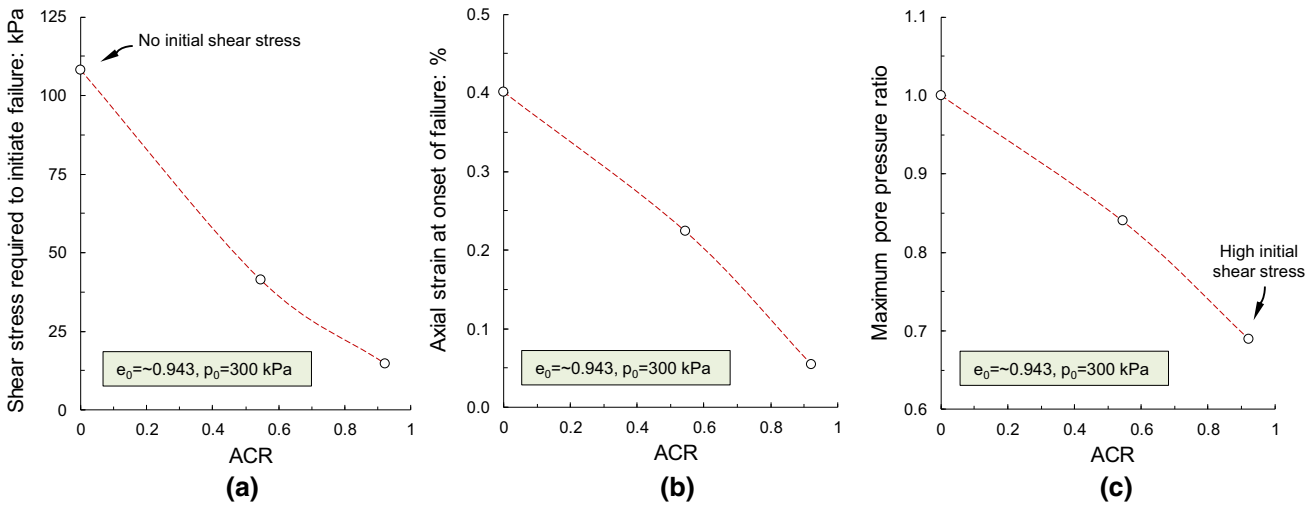

Fig. 8 Influence of initial shear stress on **a** shear stress required to initiate failure; **b** strain level at onset of instability and **c** maximum pore water pressure ratio

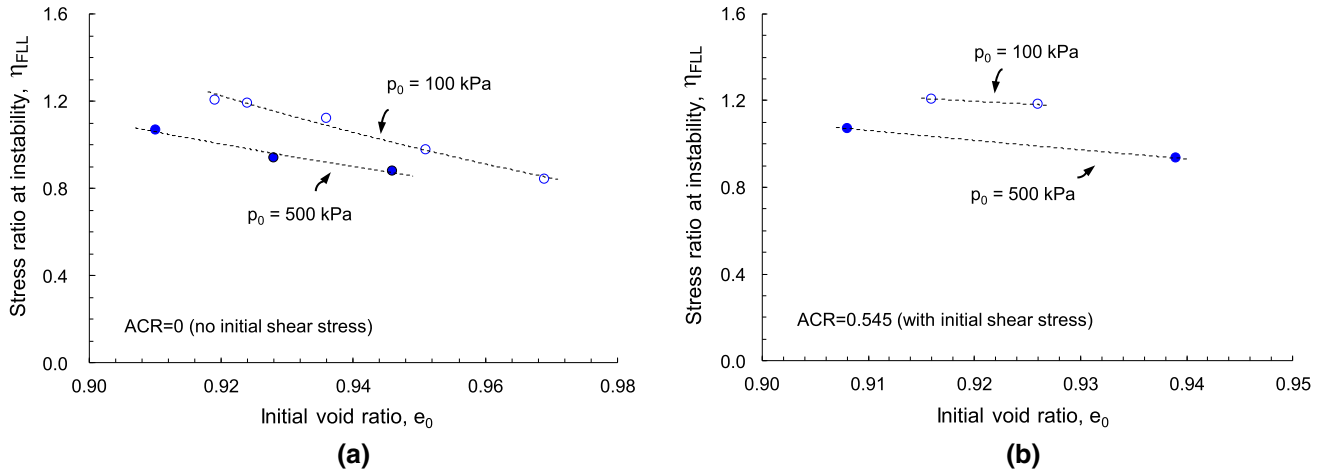

Fig. 10 State dependent stress ratio at onset of instability: **a** ACR = 0; **b** ACR = 0.545

confining stress tends to exhibit a lower stress ratio and hence is more prone to the triggering of flow liquefaction. The two important features, which have been observed on several different sands in the literature, have also been confirmed by the experiments on anisotropically consolidated specimens, as shown in Fig. 10b for the case of ACR = 0.545.

In accordance with the proposal of Yang [35], the effects of void ratio and confining stress on the flow liquefaction line in the stress space can be combined through the state parameter defined with reference to the critical state locus in the compression space. To examine whether this idea is valid for the general anisotropic consolidation conditions, the critical state data are retrieved from the experimental results. Shown in Fig. 11a is the collection of the critical states attained from all tests, including both isotropically and anisotropically consolidated specimens. Clearly, a unique straight line which fits all data very well exists, suggesting that the critical state locus is not affected by the consolidation path. The gradient of the straight line (M) is measured as 1.21, representing the angle of shearing resistance (ϕ_{cs}) of 30.1°. The uniqueness of critical state line is also confirmed in the compression plane, as shown in Fig. 11b, where a unique trend line can be proposed to fit all data reasonably well regardless of isotropic or anisotropic consolidation. The critical state line here is described by a power function as

$$e = e_\Gamma - \lambda_c \left(\frac{p}{p_a}\right)^n \tag{5}$$

where the exponent n typically takes a value of 0.6; e_Γ and λ_c are two key parameters that reflect the characteristics of soil grains such as shape and gradation [38, 39].

Based on the critical state locus determined, the slope of the flow liquefaction line (η_{FLL}) is plotted as a function of initial state parameter (ψ_0) for the case of ACR = 0 and the

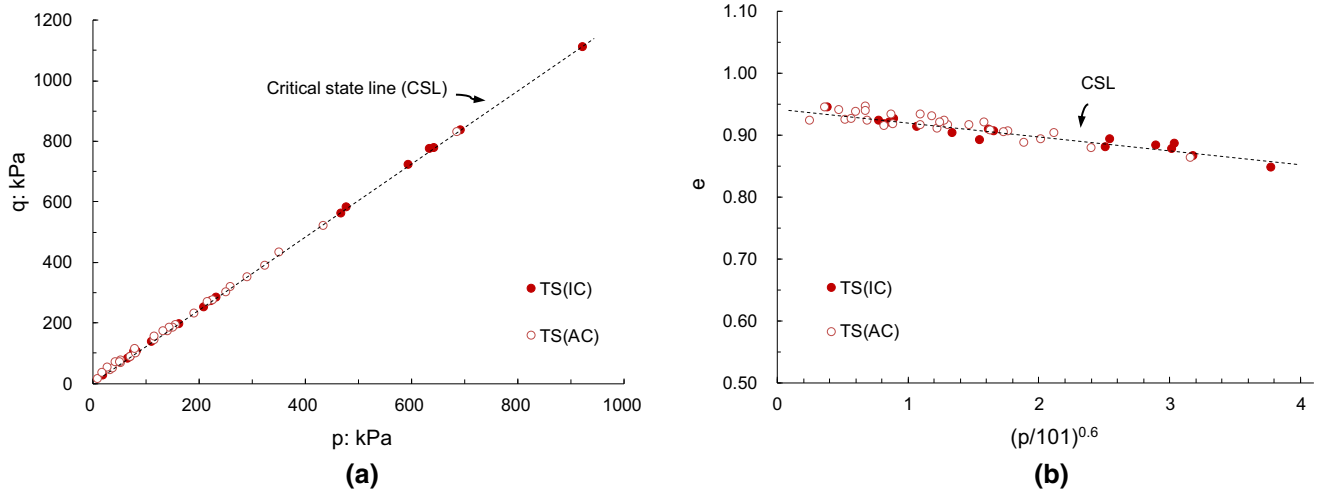

Fig. 11 Critical states of isotropically and anisotropically consolidated sand specimens: **a** *q*–*p* space; **b** *e*–*p* space

case of ACR = 0.545, respectively, in Fig. 12a, b. It is encouraging that for both cases, the effects of void ratio and confining stress observed in Fig. 10 can be unified such that a single relationship exists between η_{UIS} and ψ_0. More strikingly, when all data are plotted together, a single trend line can be proposed to fit the data reasonably well, regardless of the presence of an initial shear stress or not, as shown in Fig. 13. This result is in agreement with that of Chu and Wanatowski [7] on K0-consoildated and isotropically consolidated specimens. Note that the trend line in Fig. 13 takes the exponential form in Eq. (3), with parameters B and A determined by regression to be 1.01 and −0.51, respectively.

The finding in Fig. 13 is significant in that the state parameter dependence of the flow liquefaction line is not affected by the presence of initial static shear stress. In other words, the relationship in Eq. (3) can be determined from the conventional triaxial tests on isotropically consolidated specimens and then be applied to the general anisotropic consolidation conditions. Furthermore, the flow liquefaction line so determined can also be applied to cyclic loading conditions—an excellent example is shown in Fig. 14 where the correspondence between monotonic and cyclic loading conditions is given. Two specially designed tests on Toyoura sand are included in the figure: one was subjected to isotropic consolidation and then to undrained monotonic loading to flow failure, and the other was anisotropically consolidated to the same state in terms of void ratio and mean effective stress and then subjected to cyclic loading. It can be seen that when the cyclic stress path touched on the flow liquefaction line determined from the monotonic test, the flow-type failure was initiated in the form of abrupt runaway deformation.

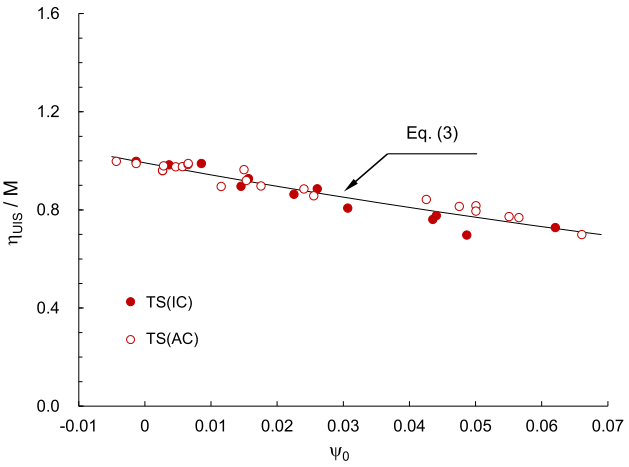

Fig. 13 Variation in stress ratio at onset of instability with initial state parameter

5 Undrained strength and factor of safety against flow failure

The potential for flow liquefaction is a critical concern in the design and construction of earth structures such as fill slopes, tailings dams and artificial islands. The conventional stability analysis in engineering practice involves calculation of the factor of safety (FS) using the internal friction angle of the soil. For loose slopes that are susceptible to liquefaction, this kind of analysis often gives sufficiently high FS values, leading to the conclusion that the slopes are safe. Caution should be exercised, however, that loose slopes with high FS values so calculated can still fail—a clear example is the collapse of the Merriespruit tailings dam in South Africa that was evaluated to have a FS as high as 1.33 [11]. There has been confusion among practicing engineers, particularly those in the mining industry.

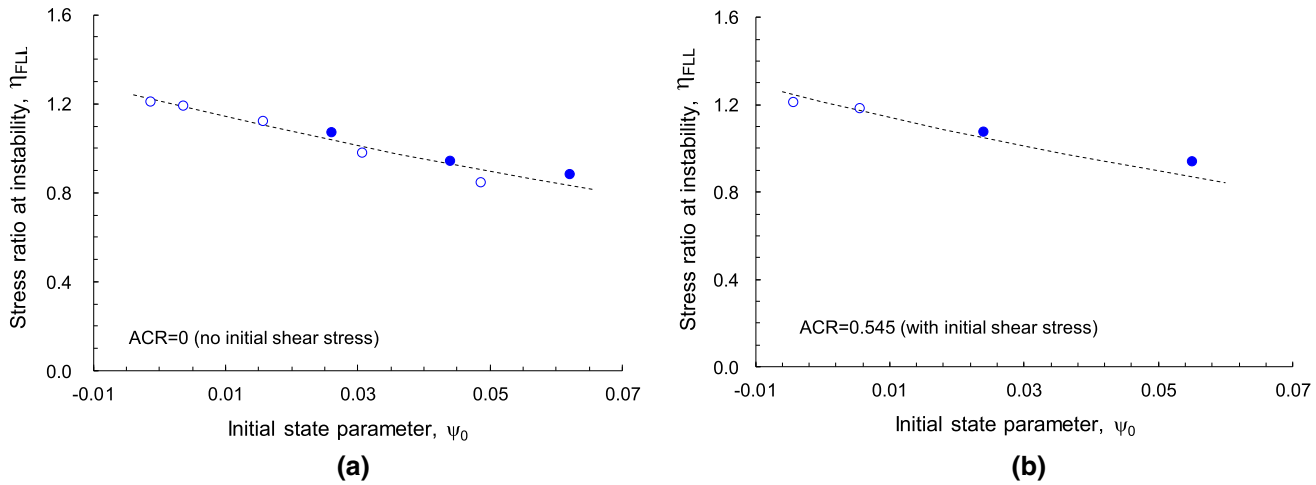

Fig. 12 State parameter dependent stress ratio at onset of instability: **a** ACR = 0; **b** ACR = 0.545

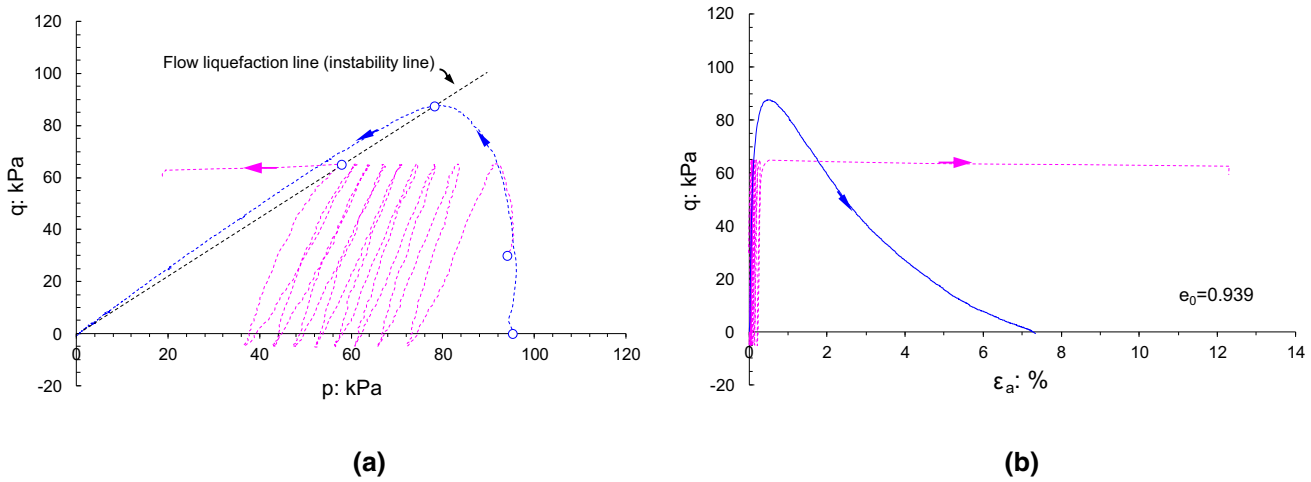

Fig. 14 Correspondence between monotonic and cyclic loading-induced flow liquefaction (after [41]: **a** stress path, **b** stress–strain relation

From the viewpoint of soil mechanics, the unreliable prediction is associated with the misconception inherent with the conventional method of stability analysis. That is, the method involving the use of the internal friction angle is essentially an effective stress-based analysis, with the assumption that the external loading is slow and no excess pore water pressure is generated during failure. Evidently, this assumption does not reflect the physics involved in flow liquefaction behavior and, hence, can lead to unsafe prediction. Based on the laboratory observations described before, an alternative method is put forward here for the evaluation of safety factor. In doing that, the typical pattern of the observed behavior is schematically shown in Fig. 15, where the element of soil is subjected to a static, driving shear stress (s_0) before undrained shear. The resistance to flow liquefaction, denoted as R_{FL}, is defined as the difference between the undrained strength (s_p) and the initial shear stress (s_0), while the difference between the undrained strength and the strength at critical state (s_u) is a measure of brittleness [2]. For an applied shear stress or perturbation (s_d), the difference between its magnitude and the magnitude of the initial shear stress represents the shear stress increment (denoted as S_{IC}) due to external loading. It is thus logical to define the factor of safety against flow failure as

$$\mathrm{FS} = \frac{R_{\mathrm{FL}}}{S_{\mathrm{IC}}} = \frac{(s_p - s_0)}{(s_d - s_0)} \tag{6}$$

The above definition takes account of three key factors governing the flow slide of a slope, namely the initial, driving shear stress, the undrained shear strength and the perturbation (i.e., a triggering mechanism). Note that the undrained shear strength here is treated as a *state parameter dependent quantity* rather than a constant, as discussed later. Since the liquefaction resistance is related to the initial shear stress in the way that it decreases with increasing ACR (Fig. 8a), a conceptual illustration for the safety factor defined in Eq. (6) is given in Fig. 16, where a

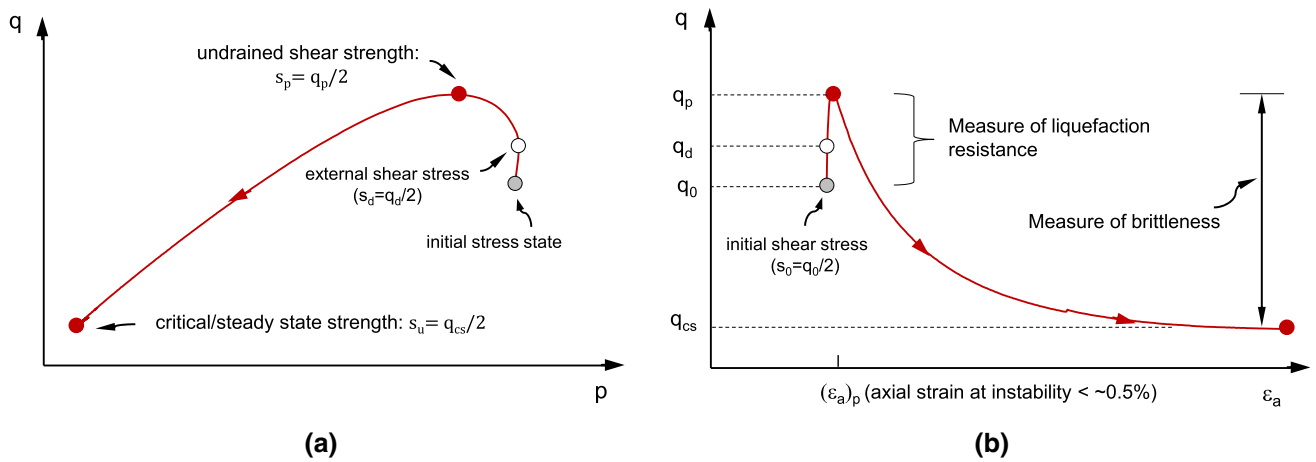

Fig. 15 Characterizing undrained shear response of loose sand in the presence of initial shear stress: **a** stress path; **b** stress–strain curve

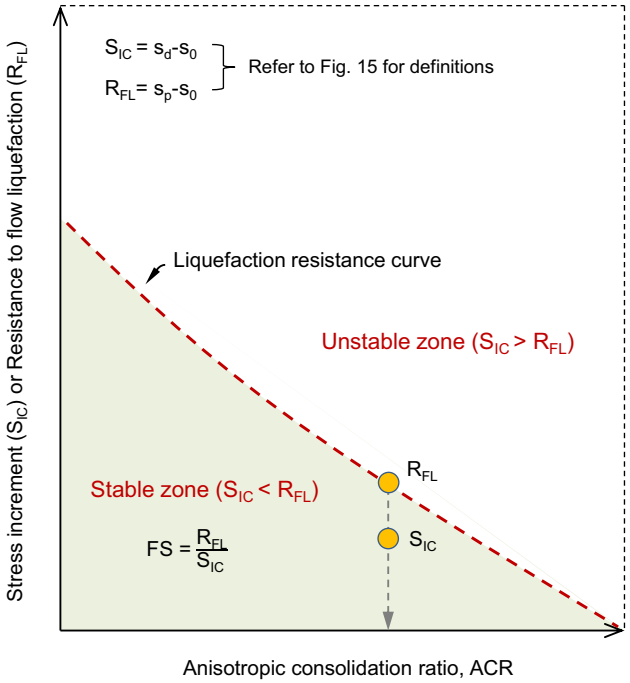

Fig. 16 Conceptual illustration for Factor of Safety against flow liquefaction

liquefaction resistance curve is shown in the R_{FL} versus ACR plane. The resistance curve serves as a demarcation between the stable zone (i.e., FS > 1) and the unstable zone (i.e., FS < 1), and for states in the stable zone the vertical distance from the liquefaction resistance curve indicates the margin of safety.

The critical issue in estimating the factor of safety is to properly determine the undrained shear strength—here the strength is that at the onset of instability rather than at the critical state. Compared with the latter, the former is considered more appropriate for safety analysis and can be determined reliably from strain-controlled tests. Figure 17 shows test results for the case of ACR = 0 and the case of ACR = 0.545, where undrained shear strength is plotted as a function of void ratio for various confining stresses. It can be seen that at a given confining stress, the undrained shear strength decreases with increasing void ratio and that at a given void ratio, the undrained shear strength increases with increasing confining stress. In geotechnical engineering practice, the undrained strength of soil is often normalized by the effective confining stress or effective vertical stress (*e.g.* [2, 22, 33]). With this notion in mind, the undrained strength here is normalized by the initial confining stress, i.e., s_p/p_0, and then plotted as a function of the initial state parameter (ψ_0), as shown in Fig. 18. A striking observation is that despite some scatter, a unique trend line can be proposed to fit the data for *both isotropic and anisotropic* conditions. The trend line can be described by an exponential function:

$$\frac{s_p}{p_0} = \alpha \exp(\beta \psi_0) \tag{7}$$

where α and β are determined by regression to be 0.60 and −10.52, respectively. The above relationship suggests that the undrained strength ratio (s_p/p_0) decreases with increasing state parameter—certainly it is a reasonable trend. For sand at very loose state (*e.g.* ψ_0 = 0.05–0.08) such that it is highly susceptible to liquefaction, Eq. (7) gives the undrained shear strength (s_p) ranging from 0.26 to $0.35p_0$. Interestingly, Olson and Stark [22] back-analyzed a number of case histories of liquefaction flow failures and showed the undrained strength ratios (with reference to the effective vertical stress) ranging from 0.24 to 0.30. While the back analyses may involve some uncertainties related to, for example, shearing mode and soil variability, the good agreement suggests the soils in these case histories being at very loose state in terms of the state parameter and hence being highly liquefiable.

Two additional points in Eq. (7) deserve attention. First, the relationship is analogous to the relationship between the peak friction angle and the initial state parameter for dense sand under drained loading [37]. Second, the above relationship together with the relationship in Eq. (3) suggests that the undrained strength ratio is related to the internal friction angle. These two points imply that while the relationships expressed in Eqs. (7) and (3) are established from experimental data, they are backed up by the constitutive theory and therefore should be applicable to a range of granular soils. Further research along this line is worthwhile and will be reported in future.

Moreover, it should be mentioned that the factor of safety defined in Eq. (6) is with reference to the undrained triaxial loading path shown in Fig. 15. This loading path represents trigger mechanisms involving rapid fill deposition or sediment accumulation as in many case histories [19, 25]. For other possible trigger mechanisms, different loading paths may be involved. For example, the slope failure induced by rising water table or rainfall infiltration can be represented by a constant shear stress path as shown as Path 2 in Fig. 19. The stability analysis of Fourier and Tshabalala [11], discussed above, actually assumed a constant-p path (Path 3 in Fig. 19). Among the three stress paths, the constant shear stress path leads to the least shear strength. Laboratory investigation of the constant shear stress path is beyond the scope of the present study; several researchers have reported interesting data (*e.g.* [6, 20]). In laboratory, a constant shear stress is often conducted in a triaxial device by applying a constant axial force while reducing the cell pressure at a slow rate and with drainage permitted. Such tests are stress controlled and hence are not able to provide reliable measurements of strain-softening response. Furthermore, the data of constant shear tests are

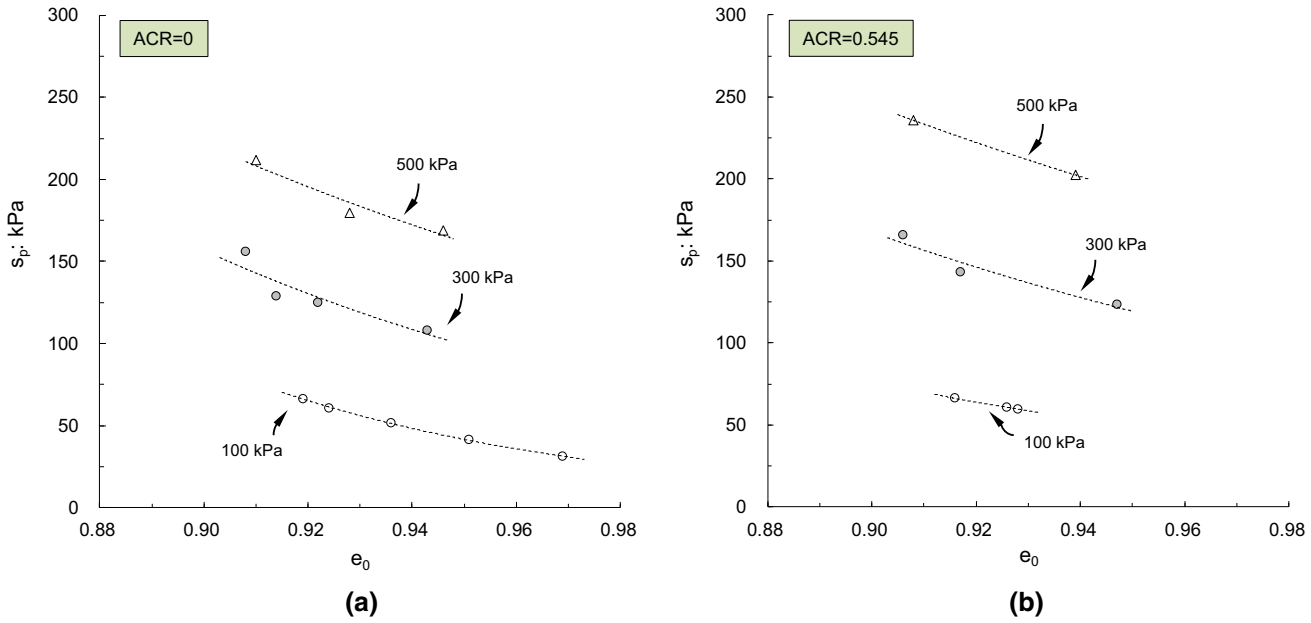

Fig. 17 State-dependent undrained shear strength: **a** without initial shear stress; **b** with initial shear stress

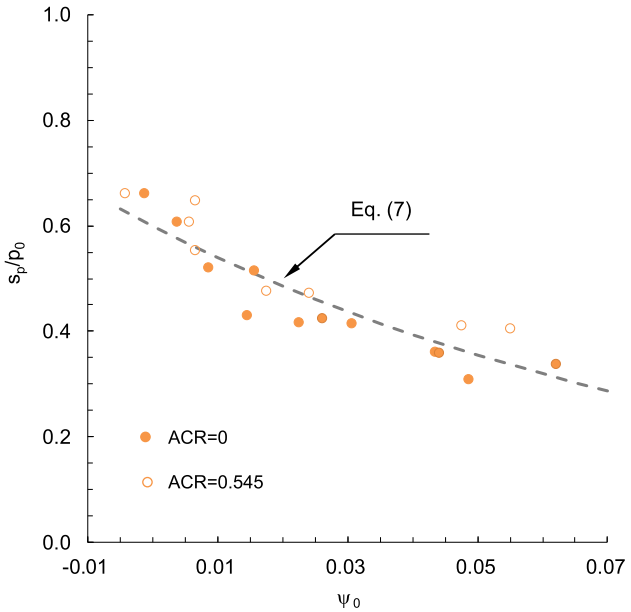

Fig. 18 Undrained shear strength ratio as a function of initial state parameter

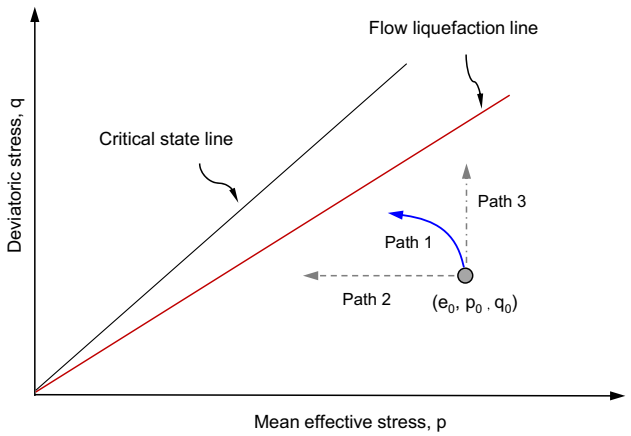

Fig. 19 Different stress paths leading to failure

often noisy with significant scatter, making the interpretation of instability initiation difficult. Future work is needed to address these limitations.

6 Summary and conclusions

This paper presents systematic datasets along with interpretation in the critical state framework to elucidate the role of initial shear stress in the initiation of instability and flow failure in granular soils. The main results and findings are summarized as follows.

(a) The flow liquefaction line or the instability line under the general anisotropic consolidation is dependent on both void ratio and mean effective stress. At a given confining stress, the gradient of the line decreases with increasing post-consolidation void ratio; whereas for a given void ratio the gradient of the line increases with decreasing confining stress. This result suggests that flow liquefaction is triggered more easily at larger void ratio and higher confining stress.

(b) The combined effects of void ratio and confining stress can be unified through the state parameter defined in the critical state theory such that the

gradient of the flow liquefaction line decreases with increasing the initial state parameter. The relationship can be well described by an exponential function, and it is almost unique irrespective of whether a static driving shear stress is present or not.

(c) Flow failure or instability can be initiated at an extremely low strain ($\sim$ 0.05%) when a significantly high initial shear stress is present. This implies that the displacements associated with the onset of flow failure of steep slopes in field conditions could be very small such that any deformation-based precautionary warning would be difficult, if not impossible.

(d) The presence of initial shear stress prevents the generation of pore water pressure under either monotonic or cyclic loading conditions. The commonly adopted liquefaction criterion in terms of pore water pressure generation can be misleading in situations where the initial shear stress is significantly large. A rapid development of large strain is considered a more rational criterion for the triggering of liquefaction.

(e) The conventional method for calculation of the factor of safety against instability is essentially an effective stress-based analysis. The assumption behind the method does not reflect the physics involved and hence can lead to unsafe predictions. The new definition for the factor of safety is established on the characteristics of the observed behavior and takes proper account of the key factors involved. It can be used as an alternative in the evaluation of the factor of safety against flow failure.

(f) The undrained shear strength together with the initial shear stress determines the resistance to flow liquefaction and thereafter the factor of safety. The undrained shear strength is not a constant, but depends on the initial state in terms of void ratio and confining stress. By normalizing the undrained strength with the mean confining stress, an almost unique relationship can be established between the strength ratio and the initial state parameter for both anisotropic and isotropic consolidation.

Last, but not the least, it should be recognized that further work to validate these findings using quality data on different materials is worthwhile. The database can be a valuable reference for validation and calibration of constitutive models and numerical simulations. Since liquefaction flow slides continue to cause extensive damage to our built and natural environment, such work is highly desirable.

Acknowledgments This work was funded by the Research Grants Council, University Grants Committee of Hong Kong (No. 17250316; 17206418). This support is gratefully acknowledged. The authors also wish to thank Mr. A Small for his constructive comments on the manuscript.

Data Availability Statement All data that support the findings of this study are available from the corresponding author upon reasonable request.

References

1. Been K, Jefferies MG (1985) A state parameter for sands. Géotechnique 35(2):99–102
2. Bishop AW (1971) Shear strength parameters for undisturbed and remoulded soil specimens. Proceedings of Roscoe memorial symposium, Henley-on-Thames: G.T. Foulis
3. Borja RI (2006) Conditions for liquefaction instability in fluid-saturated granular soils. Acta Geotech 1:211–224
4. Casagrande A (1975) Liquefaction and cyclic deformation of sands, a critical review. Proc. of 5th Pan-American conference on Soil Mech. Found. Eng., vol 5, pp 79–133
5. Chu J, Leong WK (2002) Effect of fines on instability behaviour of loose sand. Géotechnique 52(10):751–755
6. Chu J, Leong WK, Loke WL, Wanatowski D (2012) Instability of loose sand under drained conditions. J Geotech Geoenviron Eng ASCE 138(2):207–216
7. Chu J, Wanatowski D (2008) Instability conditions of loose sand in plane strain. J Geotech Geoenviron Eng ASCE 134(1):136–142
8. Dai BB (2010) Micromechanical investigation of the behavior of granular materials. Ph.D. thesis, The University of Hong Kong
9. Dai B, Yang J, Luo X (2015) A numerical analysis of the shear behavior of granular soil with fines. Particuology 21:160–172
10. Doanh T, Ibraim E, Matiotti R (1997) Undrained instability of very loose Hostun sand in triaxial compression and extension Part 1: experimental observations. Mech Cohes-Frict Mater 2(1):47–70
11. Fourie AB, Tshabalala L (2005) Initiation of static liquefaction and the role of K_0 consolidation. Can Geotech J 42(3):892–906
12. Hill R (1958) A general theory of uniqueness and stability in elastic-plastic solids. J Mech Phys Solids 6:236–249
13. Huang X, O'Sullivan C, Hanley KJ, Kwok CY (2014) Capturing the state-dependent nature of soil response using DEM. In: Geomechanics from micro to macro, CRC Press
14. Ishihara K (1993) Liquefaction and flow failure during earthquakes. Géotechnique 43(3):351–451
15. Ishihara K (1996) Soil behaviour in earthquake geotechnics. Oxford Scientific Publications
16. Jefferies MG, Been K (2016) Soil liquefaction: a critical state approach. Taylors & Francis
17. Keramatikerman M, Chegenizadeh A, Nikraz H, Sabbar AS (2018) Effect of fly ash on liquefaction behavior of sand-bentonite mixture. Soils Founds 58(5):1288–1296
18. Kramer SL, Seed HB (1988) Initiation of soil liquefaction under static loading conditions. J Geotech Eng 114(4):412–430
19. Lade PV (1993) Initiation of static instability in the submarine Nerlerk berm. Can Geotech J 30(6):895–904
20. Monkul MM, Yamamuro JA, Lade PV (2011) Failure, instability, and the second work increment in loose silty sand. Can Geotech J 48:943–955
21. Morgenstern NR (2017) The evaluation of slope stability: a further 25 year perspective. HKIE Distinguished Lecture, The Institution of Hong Kong Engineers
22. Olson SM, Stark TD (2003) Yield strength ratio and liquefaction analysis of slopes and embankments. J Geotech Eng Div ASCE 129(8):727–737

23. Poulos SJ, Castro G, France JW (1985) Liquefaction evaluation procedure. J Geotech Eng Div ASCE 111(6):772–792
24. Rahman M, Lo SR (2011) Predicting the onset of static liquefaction of loose sand with fines. J Geotech Geoenviron Eng ASCE 138(8):1037–1041
25. Sladen JA, D'Hollander RD, Krahn J (1985) The liquefaction of sands, a collapse surface approach. Can Geotech J 22(4):564–578
26. Sze HY, Yang J (2014) Failure modes of sand in undrained cyclic loading: Impact of sample preparation. J Geotech Geoenviron Eng ASCE 140(1):152–169
27. Vaid YP, Chung EFK, Kuerbis RH (1990) Stress path and steady state. Can Geotech J 27:1–7
28. Vaid YP, Eliadorani A, Sivathayalan S, Uthayakumar M (1999) Quasi-steady state: a real behavior: discussion. Can Geotech J 36(1):182–183
29. Verdugo R, Ishihara K (1996) The steady state of sandy soils. Soils Founds 36(2):81–91
30. Wanatowski D, Chu J (2007) Static liquefaction of sand in plane strain. Can Geotech J 44(3):299–313
31. Wei LM, Yang J (2014) On the role of grain shape in static liquefaction of sand-fines mixtures. Géotechnique 64(9):740–745
32. Wood DM (1990) Soil behaviour and critical state soil mechanics. Cambridge University Press
33. Wroth CP (1984) The interpretation of in situ soil tests. Géotechnique 34(4):449–489
34. Yamamuro JA, Lade PV (1997) Static liquefaction of very loose sand. Can Geotech J 34(6):905–917
35. Yang J (2002) Non-uniqueness of flow liquefaction line for loose sand. Géotechnique 52(10):757–760
36. Yang J, Dai BB (2011) Is the quasi-steady state a real behaviour?—A micromechanical perspective. Géotechnique 61(2):175–184
37. Yang J, Li XS (2004) State-dependent strength of sands from the perspective of unified modeling. J Geotech Geoenviron Eng ASCE 130(2):186–198
38. Yang J, Luo XD (2015) Exploring the relationship between critical state and particle shape for granular materials. J Mech Phys Solids 84:196–213
39. Yang J, Luo XD (2018) The critical state friction angle of granular materials: does it depend on grading. Acta Geotech 13(3):535–547
40. Yang J, Sze HY (2011) Cyclic behaviour and resistance of saturated sand under non-symmetrical loading conditions. Géotechnique 61(1):59–73
41. Yang J, Sze HY (2011) Cyclic strength of sand under sustained shear stress. J Geotech Geoenviron Eng ASCE 137(12):1275–1285
42. Yang J, Wei LM (2012) Collapse of loose sand with the addition of fines: the role of particle shape. Géotechnique 62(12):1111–1125
43. Zhang H, Garga VK (1997) Quasi-steady state: a real behavior? Can Geotech J 34(5):749–761